WARNING. This material may be protected by copyright law
(title 17 U.S. code)

Purdue University Interlibrary Loan (IPL)

ILLiad TN: 636288

ILL Number: 35851199

Call #: 620.505 J826

Location: PHYS

ARIEL
Charge 15
Maxcost: 50.00IFM

Borrower: CUV
Aging Date: 20071009
Transaction Date: 10/10/2007 04:01:39 PM

Lending String: *IPL,ITD,MYG,UUM,TXH

Patron: DU, Chunsheng (Faculty [dds])

Journal Title: Journal of Computational and Theoretical Nanoscience

Volume: 3 **Issue:** 4
Month/Year: 2006

Pages: 506-512

Article Author:

Article Title: Zhong, W \ Modeling liquid transport in fibrous structures; An multi-scale approach

Imprint: American Scientific \ Stevenson Ranch, C

Shipping Address:
University of California, Davis
ILL/ Shields Library
100 NW Quad
Davis CA 95616-5292

Fax: 530 752-7815
Ariel: 169.237.75.50

COPY PROBLEM REPORT

Purdue University Libraries Interlibrary Loan Department (IPL)

Ariel: 128.210.125.135
Fax: 765-494-9007
Phone: 765-494-2805

Please return this sheet within **5 BUSINESS DAYS** if there are any problems.

_____ Resend legible copy

_____ Wrong article sent

_____ Other, explain _____

DOCUMENTS ARE DISCARDED AFTER 5 DAYS. PLEASE RESUBMIT REQUEST AFTER THAT TIME.

Copyright © 2006 American Scientific Publishers
All rights reserved
Printed in the United States of America

Journal of
Computational and Theoretical Nanoscience
Vol. 3, 506–512, 2006

RESEARCH ARTICLE

Modeling Liquid Transport in Fibrous Structures: An Multi-Scale Approach

Wen Zhong[1], Ning Pan[2,*], and David Lukas[3]

[1] *Department of Textile Sciences, University of Manitoba, Winnipeg, MB R3T 2N2, Canada*
[2] *Department of Biological and Agricultural Engineering, University of California, Davis, CA 95616, USA*
[3] *Technical University of Liberec, Liberec, Czech Republic*

The Ising model combined with Kawasaki dynamics is applied in modeling liquid transport in fibrous materials. This meso-scale approach is especially useful in the study of materials with characteristic length scale in the range of nano- and micrometers, where conventional continuum mechanics approach is no longer valid. The technique presented in this paper represents an attempt for cross-scale modeling of physical phenomena to bridge the gap between macro behavior of a heterogeneous material system and those of its basic constituent particles. The transition from one scale to another is carried out by the so called "hand-shaking strategy."

Keywords: Multi-Scale Modeling, Liquid Transport, Fibrous Materials, Ising Model.

1. INTRODUCTION

As a classic topic with its application in the field of fiber processing and fiber composite manufacturing, liquid transport in fibrous materials has attracted research interests for a long time. Yet its latest applications in such critical areas as nano-fibrous materials for absorption, biofiltration, and purification prompt for more precise and efficient methods in studying and analyzing related physical mechanisms.

Non-homogeneous flow has been an active area for research since 1970s, when some pioneering works on dynamics of liquid spreading on solids had been published, e.g., Huh and Scriven (1971) suggested a singularity in the dissipation in such flows. Later, a distinction was found between the behavior of a simple fluid, which spreads by a "rolling motion" (Dussan and Davis (1974)), and that of a polymeric melt, which often tend to slip on a solid surface (Brochard and de Gennes (1984)). De Gennes (1985) also published a reviewing work on wetting.

As to fibrous materials, an even earlier attempt to understand capillary driven non-homogeneous flows was made by Lucas (1918) and Washburn (1921). Lucas-Washburn (LW) theory has since been used in studying wicking/wetting phenomena in fibrous media. Chatterjee (1985) dealt with such flow during dyeing process. Pillai et al. (1996) experimented on capillary driven flow of viscous liquids across aligned fibers. Hsieh (1995) discussed wetting/wicking theories and their applications to liquid transport in fibrous materials. Lukas et al. (1999) tested the validity of LW equation and proposed a revision with the account of gravity. More recently, Starov et al. (2003) studied the spreading of small liquid drops over thin and thick porous layers in the case of both complete wetting and partial wetting, accounting for such effects as lubrication, permeability, and capillary pressure.

Before 1990's, most efforts in dealing with flow in fibrous media were based on macroscopic phenomenon and adopted to a large degree empirical methods. A new approach in studying non-homogeneous flows using stochastic simulation has been developed in the past decades. Manna et al. (1992) presented a 2D stochastic simulation of the shape of a liquid drop on a wall due to gravity. The simulation was based on the combination of the so called Ising model and Kawasaki dynamics. Lukkarinen (1995) studied the mechanisms of fluid droplet spreading on flat solids using a similar model. However, these work dealt only with flow problems in a flat surface instead of a real heterogeneous structure. Only recently is the Ising model used in the simulation of wetting dynamics in heterogeneous fibrous structures (Lukas et al. (1997) and Zhong et al. (2002)).

In this paper, the Ising model combined with Kawasaki dynamics, a so called "meso-scale" approach, is further extended to both a larger scale and a smaller scale to bridge the gap between macro behavior of a heterogeneous material system and those of its basic constituent particles, resulting in an attempt of cross-scale modeling of

*Author to whom correspondence should be addressed.

1546-198X/2006/3/506/007 doi:10.1166/jctn.2006.006

the problem. The transition from one scale to another is carried out by the so called "hand-shaking strategy," that is, the information gained from a lower scale is summed into a finite set of parameters, and passed onto a higher scale. This attempt is to provide a useful tool in study material system with characteristic length scales over the range of micro- and nano-meters.

2. MODEL DESCRIPTION

2.1. The Ising Model

In statistical thermodynamics, the macro characteristics of a system are always a reflection of interactions and resulting balance among microparticles or cells that comprise the system. In the original Ising model, accordingly, a one-dimensional system is divided into a number of lattice cells. Then the Hamiltonian is calculated as the summation of the interactions between each pair of the nearest neighboring cells. And the average macroscopic parameters of the system can be derived from the Hamiltonian via methods in statistical mechanics. Advantage of the Ising model is that, due to its simple expression, it can be used to describe a complex system made of subsystems with two interchangeable configurations, i.e., by "digitalizing" the original system into a grid of cells with state 1 or 0 only.

In a two-dimensional Ising model for liquid transport, the field is divided into a lattice frame of L × M square of cells, as shown in Figure 1. Two variables are used in the model to describe the state of each cell in the lattice:

(i) s is used to describe whether a cell is occupied by liquid denoted as 1 or 0 otherwise. In the simulation, liquid can move from one cell to another, as in real transport process of liquid in media.

(ii) F is used to describe whether a cell is occupied by the fibrous medium, taking either 1 (a cell with fibers) or 0 (a cell without fiber). For simplicity, fibers are assumed to be free from moving during the simulation.

The total Hamiltonian of the system, H, is considered as a sum of all the contributions of the cell energies in the lattice. When only the interactions between nearest neighbors are considered, the Hamiltonian for an arbitrary cell i can be expressed as

$$H_i = -\left(B_0 \sum_i s_i F_i + B_1 \sum_{i,j} s_i F_j\right) - C \sum_{i,j} s_i s_j + G \sum_i s_i y \quad (1)$$

where the first term in the bracket represents the interactions between liquid and fiber substrate spins that coexist in one cell, while the second term represents those between neighboring cells, and the coefficients B_0 and B_1 are the adhesive energy of interaction between fiber and liquid. The second term in the RHS of Eq. (1) indicates the interactions between the liquid spins, and C is the cohesive energy of the liquid. The last term reflects the energy of liquid spins in the gravitational field, of which G is the intensity of the gravity field and y the y-coordinate of a cell in the lattice. Interactions of longer distance terms can be incorporated when necessary, e.g., second nearest neighbors and third neighbors in (Lukas et al. (1997)).

This 2-D model can be easily expanded into a 3-D one, in which the number of nearest neighbors increased from 8 to 26, as shown in Figure 2.

2.2. The Kawasaki Dynamics

The evolution of the system is directed by minimization of the system Hamiltonian, H, expressed in Eq. (1), and the minimization of H is based on descent steps caused by spin exchanges that obey the Kawasaki dynamics (Abraham and Newman (1988)). Let us consider a thermodynamics system connected with a thermodynamics reservoir, and energy exchange can occur between them. The system together with the reservoir forms a canonical assembly that is governed by the Boltzmann distribution of the state probability ratio (Lukas (2003)), i.e.,

$$\frac{P(H_a)}{P(H_b)} = \Lambda = \exp\left(-\frac{\Delta H}{\tau}\right) \quad (2)$$

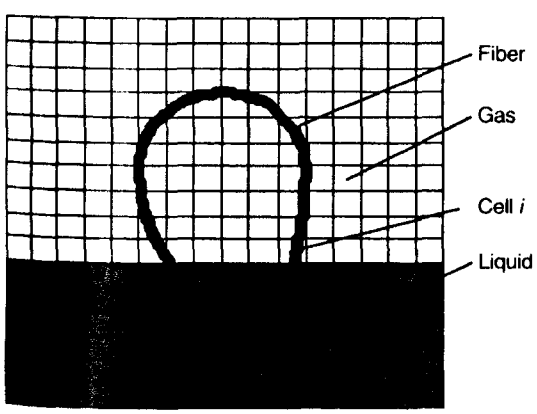

Fig. 1. A 2-D Ising model.

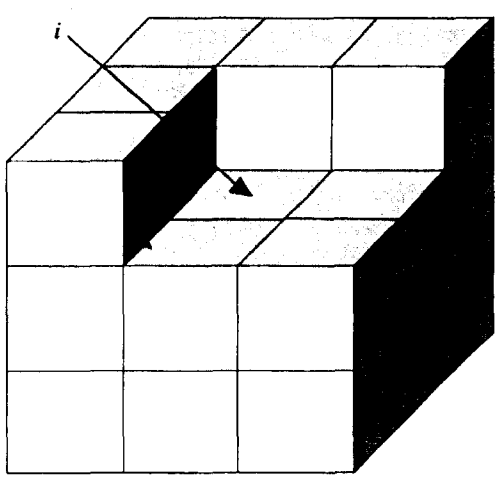

Fig. 2. A cell i in a 3-D Ising model with its neighbours.

where parameter τ is proportional to the absolute temperature. $P(H_k)$, ($k = a$ and b) is the probability that the system exists in a configuration with energy H_k. Λ is then a measure of the probability for the system to change its configuration, through spin exchange, from a state with energy H_a to a state with energy H_b. The energy difference ΔH is the change of the total system energy before and after the spin exchange.

More specifically, two randomly chosen spins i and j of different spin values +1 and 0 are considered. The system Hamiltonians H_a and H_b are calculated for cases before (H_a) and after (H_b) the spin value exchange. A random number r is then chosen from the interval [0, 1] as spin exchange probability. In the case r is less than the energy barrier ($r < \Lambda$), these two spins will exchange their position.

A more detailed discussion on the Kawasaki dynamics can be found from our previous paper (Lukas et al. (1997)). The technique involving generation of random number is the Monte Carlo method.

2.3. Simulation Algorithm

In all the simulations introduced in the present study, for simplicity, swelling/movement of fibers is neglected, that is, the values of F for all the cells remain constant. Therefore, the process of a liquid penetration in fibrous structures is the results of the liquid occupying empty spaces between fibers as well as wetting fibers. The general procedures of the simulation are as follows:

(i) Initial configuration is created by developing the lattice, above which the fibrous media is laid. The initial values of both F (1 or 0) and s (1 or 0) for each cell are also determined. A cell i is considered to be covered with fiber ($F = 1$) if the distance between the cell center and the fiber axis is smaller than the fiber radius. A number of cells near inlet port is so defined that their s values are always +1, indicate that there is a constant influx of liquid.

(ii) Scanning the liquid–fiber interface. A cell i in the lattice is randomly selected. If there is one or more nearest neighbor cells whose values of s are different from cell i, cell i is then supposed to be on the interface. As shown in Figure 1, the dry cell i is next to three liquid cells and five dry cells, each liquid cell having the opportunity to exchange spin values with cell i, but with different probabilities.

(iii) Cell i can be paired with each of the three liquid cells, respectively. For each pair, ΔE_T, the energy difference between configurations before and after the two cells exchange their spin values, can be calculated. And the pair with the lowest value of ΔE_T is selected as the most probable exchange.

(iv) The Monte Carlo process is applied to determine if the exchange will actually occur. One whole iteration ends when all the cells at current fluid–fiber interface have been scanned. The time required to complete the iteration is called one Monte Carlo step (MCS), a relative time scale.

(v) Repeat step (ii) to start a new round until the entire simulation is terminated.

3. MULTI-SCALE MODELING OF LIQUID TRANSPORT IN FIBROUS MATERIALS

A statistical mechanics approach like the Ising model, also known as a "meso-scale" approach, is functioned to bridge the gap between the behavior of a material at macro scale and the behaviors and interactions of its constituent micro-components. In other words, the macro behavior of a material can be predicted from the micro-interactions of its basic particles by a hierarchy modeling approach with descending scales, also known as multi-scale modeling.

This multi-scale modeling is especially useful in the study of materials with characteristic length scale over the range of nano- and micro-meters, as it is reported that there is limitations of conventional continuum mechanics approach (e.g., the finite element method) to describe the behavior of materials at scales smaller than tens of micros (Ghoniem et al. (2002)).

At the present time, a truly seamless multi-scale approach for computer simulation is still pending. As a result, the transition from one scale to another is usually carried out by a so called "hand-shaking strategy" (Goddard III et al. (2001)), that is, the information gained from a lower scale is summed into a finite set of parameters, and passed onto the higher scale.

In the following section, an attempt of multi-scale modeling of transport in fibrous materials is presented, going through from quantum field theory to statistical mechanics, and then back to continuum methods.

3.1. From Quantum Field Theory to Statistical Mechanics

The coefficients, B_0, B_1, and C in Eq. (1), that are essential to the function of the Ising model, are determined in a manner described as follows.

We assume that the Van der Waals forces dominate the interactions between fiber and liquid, as they are the ubiquitous interactions across such interfaces. Other interactions, like electrostatic forces, acid/base interactions, could be significant in some materials/liquid systems, are negligible here.

According to the Lifshitz theory (Israelachvili (1985)), the interaction energy per unit area between two surfaces can be expressed as

$$W_{1,2} = \frac{-h_{1,2}}{12\pi D^2} \tag{3}$$

where $h_{1,2}$ is the Hamaker constant and D the distance between the surfaces. Derived from the quantum field theory, an approximate expression for the Hamaker constant

Table I. Specifications of PP yarn samples.

Sample	Yarn count (tex)	Diameter of yarn (mm)	Filament fineness (dtex)	No. of filaments in a yarn	Diameter (μm)	Total surface area of fiber in a single cell (mm^2)
1	13.4	0.282	2.25	60	18	0.956
2	13.4	0.290	1.5	90	14.6	1.197
3	13.4	0.322	0.6	224	9.2	2.084

of two bodies (1 and 2) interacting across a medium 3, none of them being a conductor, is

$$h_{1,2} = \frac{3hv_e(n_1^2-n_3^2)(n_2^2-n_3^2)}{8\sqrt{2}(n_1^2+n_3^2)^{1/2}(n_2^2+n_3^2)^{1/2}\{(n_1^2+n_3^2)^{1/2}+(n_2^2+n_3^2)^{1/2}\}} + \frac{3}{4}k_BT\frac{\varepsilon_1-\varepsilon_3}{\varepsilon_1+\varepsilon_3}\frac{\varepsilon_2-\varepsilon_3}{\varepsilon_2+\varepsilon_3} \quad (4)$$

where h is the Planck's constant, v_e is the main electronic adsorption frequency in the UV range (assumed to be the same for the three bodies, and typically around 3×10^{15} s^{-1}), and n_i is the refractive index of phase i, ε_i is the static dielectric constant of phase i, k_B is the Boltzmann constant, and T the absolute temperature. Also define

$$k_1 = \frac{B_1}{C} = \frac{W_{1,2}}{W_{1,1}} = \frac{h_{1,2}}{h_{1,1}}, \quad k_2 = \frac{B_0}{B_1} = \frac{W_{1,2}\pi dal}{W_{1,2}a^2} = \frac{\pi dl}{a} \quad (5)$$

The constants k_1 and k_2 are used to represent the ratios of B_1/C and B_0/B_1, respectively.

The ratio B_0/B_1 is equal to the ratio of adhesive surface areas in each case. The area for coefficient B_0 calculated as the total surface of l individual filaments (cylindrical with diameter d) in the yarn, assuming that filaments within a yarn are evenly packed and straight along the axis of the yarn, and the area for coefficient B_1 is calculated as the area of the cell (with side length a).

The value of B_1 is determined by simulation to accommodate the experimental data, and the values of C and B_0 are determined by Eq. (5).

To testify the validity of the model, a set of wicking experiments were performed. Test samples included three types of weakly twisted polypropylene filament yarns with the same diameter but different fineness of constituent filaments. Their specifications are listed in Table I. Each sample was hung vertically by a clamp and the free end was dipped into a bath containing 1% solution of methylene blue. The traveling height of the liquid was measured during wicking tests. To obtain the wetting rate, the time required for the dye solution to travel upwards along the sample was recorded.

In the simulation, the plane is divided into 9×150 square cells. For the convenience of calculating the weight of the liquid in a cell and the interfacial area between two cells, each cell is supposed to be a cubic. The wicking experiments were performed on weakly twisted polypropylene filament yarns. Weak twists were used to maintain the rounded shape and evenness of yarn cross-sections along the lengthwise direction, so that in the simulation, a filament yarn can be represented as a fibrous assembly with even diameter: The width of a cell is made equal to the diameter of the yarn in each case. Next the weak twists pack the fiber assemblies so as to provide large number of capillaries (interstices between filaments) in the lengthwise direction as wicking channels. The weak twists also enable the simulation to depict the fiber lay out as parallel to yarn axis in each cell.

Table II. Parameters for fiber and liquid at room temperature (Krigbaum and Dawkins 1975).

	ρ (g/cm^3)	γ_{lg} 10^{-3} N/m	γ_{fg} 10^{-3} N/m	n_i	ε_i	θ
PP	0.905	—	29.4	1.490	2.2	86°
Water	0.998	72.75	—	1.333	80	

Polypropylene fiber, a material with little moisture absorbency capacity, was chosen to eliminate any shape change (i.e., swelling) of individual filaments during the experiments. As a result, the surface area of fibers is assumed to be constant during the simulation. The dominant factor for the reported wicking tests, therefore, is the structural differences between the filament yarns with the same thickness made of constituent filaments of different diameters. Hence the Ising model is significant in describing the liquid transport process in such a system.

The seed of the random number is set to be 0 at the beginning of each simulation to make the simulation repeatable. Let each Monte Carlo step (MCS) represents the relative time. The parameters needed in the simulation are listed in Table II. The experimental as well as the simulation results of the wetting rate are shown in Figure 3

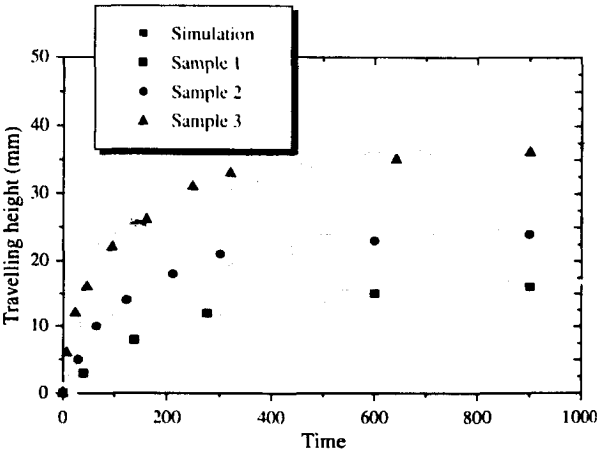

Fig. 3. Traveling height of liquid versus relative time.

(Zhong (2001)). The constant B_1 is chosen as 3.72. The constants k_1 and k_2 are calculated by Eq. (5) as: $k_1 = 1.34$, $k_2 = 12.0$ (sample 1); $k_2 = 14.2$ (sample 2); $k_2 = 20.1$ (sample 3).

Results of experiments and simulations show considerable accordance. Keeping the yarn thickness as constant, with the decrease of filament diameter and thus the increase of filament number in the yarn, the total surface area of a unit length of the yarn increases, which in turn causes an increase in the interaction area of fiber/liquid and thus in the interaction energy, resulting in a higher wettability of the yarn. This outcome also agrees well with the phenomenological studies reported in various references.

Both the experiments and simulations show that traveling height rises substantially at first and then slows down, asymptotically approaching a plateau where the effect of the gravity of the liquid column becomes significant; thus justified the introduction of gravity term into the expression of Hamiltonian.

3.2. From Statistical Mechanics to Macro Properties of Fibrous Materials

Next is a simulation on the influence of fiber orientation on the dynamics of liquid wetting/wicking in a fibrous mass using the approach described above. Fiber declination β from the vertical axis is varied with a step of 10°, so the simulation was carried out for 11 different fibrous systems with $\beta = 0°$, 10°,..., 90°, plus $\beta = 45°$. This parametric study for different angles β is to show how the present approach can be used to investigate fiber systems with different structural features (orientations, for example).

Results are provided in Figure 4 where each picture is a pair of wetting patterns of two cross sections of side and top views respectively, of the fibrous mass at a given orientation β. The horizontal cross-sections (top view) are all cut at the distance of 100 cells from the liquid surface.

Two extreme behaviors can be seen. The first is the one vertical to the W–L plane or $\beta = 0°$ where the ascending liquid moves at a highest rate but is most scattered. The other one is in parallel with the W–L plane or $\beta = 90°$ with the lowest wetting rate, but the liquid pattern is most heavily aggregated.

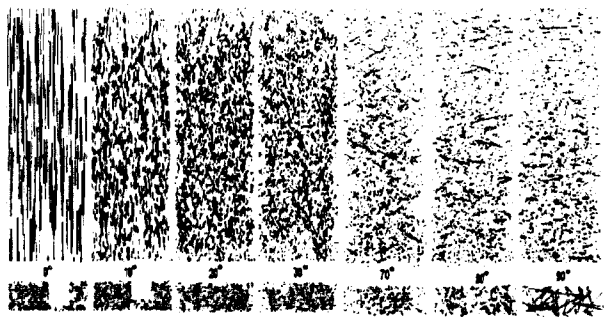

Fig. 4. Wetting patterns (vertical and horizontal cross-sections) of a fiber mass with different β after 600 MCS.

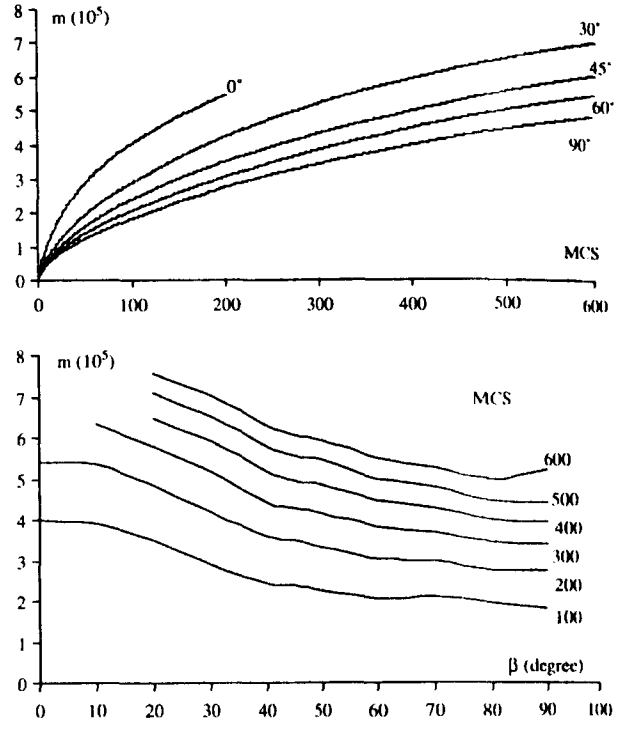

Fig. 5. (a) Liquid taken by specimen versus MCS. (b) Liquid taken by specimen versus β.

Figure 5 gives the simulated relationship of mass m (number of liquid cells) absorbed by fiber versus (a) time (Monte Carlo steps, MCS) and (b) orientation β, respectively. It is clear that after a short time, i.e., MCS < 200, the absorbed liquid body in general is more voluminous for a smaller angle β because, the fiber assemblies with smaller β values start with greater wicking rates and therefore the liquid climbs faster. Nevertheless, this trend remains true in our calculation only for those with $\beta \geq 20°$. For cases $\beta < 20°$, the climbing of the liquid will stagnate and become independent of the time; the smaller the β value, the earlier the climbing stops.

The discussions above reveal that there will be one or a range of optimal combinations of β and MCS at which the fiber mass will absorb maximum amount of liquid, a result of optimal wicking rate and wicking duration as shown in Figure 5(b); when $\beta = 20°$, the greater the MCS value, the more liquid absorbed.

To transfer these simulation results into macro parameters of the fibrous materials, such as liquid wicking rate, a modified version of LW equation is applied, as expounded below:

Classic Lucas-Washburn (LW) theory describes the liquid's velocity, dh/dt, moving up in a vertical capillary with radius r:

$$\frac{dh}{dt} = \frac{r\gamma\cos\theta}{4\mu h} - \frac{r^2\rho g\cos\beta}{8\mu} \tag{6}$$

Parameters included in the equation are contact angle θ, angle between capillary axis and vertical direction β,

viscosity of liquid μ, surface tension γ, density of liquid ρ, and gravity g.

For a given system, the LW equation can be reduced by introducing two constants

$$K' = \frac{r\gamma\cos\theta}{4\mu} \quad \text{and} \quad L' = \frac{r^2\rho g\cos\beta}{8\mu}, \tag{7}$$

into a simplified version

$$\frac{dh}{dt} = \frac{K'}{h} - L' \tag{8}$$

Equation (8) can be modified by replacing the distance h with liquid mass uptake m, as

$$\frac{dm}{dt} = \frac{K}{m} - L \tag{9}$$

The new constants K and L are

$$K = (wT\rho V_L)^2 K', \quad L = wT\rho V_L L' \tag{10}$$

where V_L is the liquid volume fraction inside the substrate of width w.

The parameter K can be used as a measure of the wicking rate in a fabric hung vertically. The values of K and L can be derived from the slope and intercept of dm/dt versus $1/m$. Note that the unit of K in real experiments in SI unit system is kg^2/sec. For computer simulation however we us mass unit [m.u.] and time step [t.s.] instead of kg and sec so that the unit for K becomes [m.u.^{2}/t.s.] (mass unit squared divided by time step).

To evaluate the wicking rate K in the simulation shown in Figures 4 and 5, time derivation of the wicked liquid mass, dm/dt, is plotted against $1/m$ with different β values in Figure 6. K could be determined from the slop of the plot as indicated in Eq. (9). In general a wicking rate can be defined as $K = tg\alpha$, where α is the slope of the plot.

It is clear from the Figures 6(a), (b), and (c) that a fibrous mass with a smaller β value does yield a higher slope or a greater wicking rate K. However, according to Eq. (9), when other parameters are given, this dm/dt against $1/m$ should be that straight line. The results of the simulation in Figure 6, which is consistent with the experimental practice, demonstrate otherwise. In reality, the wicking rate K cannot maintain a constant because among other factors the liquid weight will slow down and eventually stop the wicking process, i.e., the wicking rate K decreases monotonically with time until levels off.

This comparison between the analytical result based on Washburn equation (continuum mechanics approach) and the simulations of the Ising model and Monte Carlo method (meso-scale approach) indicates that the latter results better represent the experimental observations. This also provides a strong evidence for validating our computer simulation method: That the meso-scale approaches are more powerful than continuum methods in dealing with problems with complicated structures in micro/nano scales.

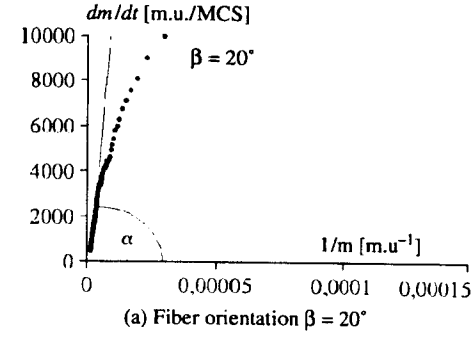

(a) Fiber orientation β = 20°

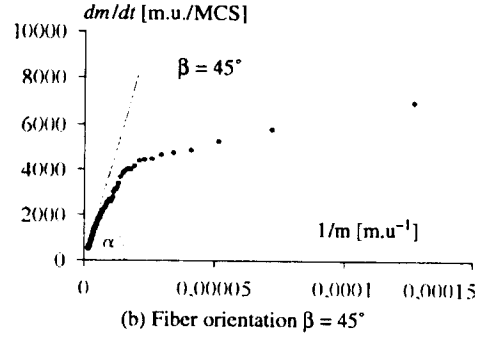

(b) Fiber orientation β = 45°

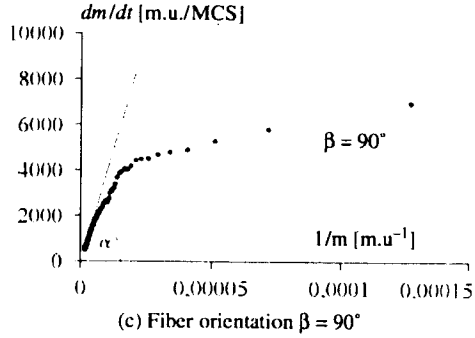

(c) Fiber orientation β = 90°

Fig. 6. Time derivation of wicked liquid mass, dm/dt, against the reciprocal mass $1/m$. The straight line—LW equation; dotted line—computer simulation.

A more complete analysis of the relationship between wicking rate K and the fiber mass orientation angle β based on the simulated data is summarized in Figure 7. We see the relations between them is also non-linear, with rapid decrease of K in the interval $\beta \sim (0°, 30°)$, while the rest of the graph, $\beta > 30°$, showing a constant or even slight increase of K.

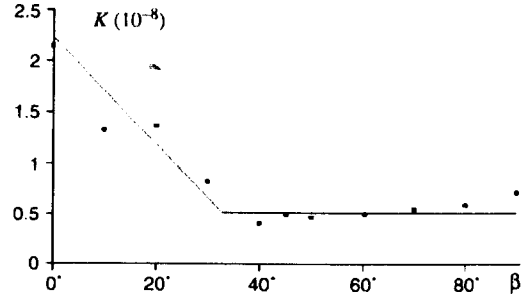

Fig. 7. The generalised wicking rate K versus β.

4. CONCLUSION

A meso-scale approach, the Ising model combined with Kawasaki dynamics, is applied in the study of liquid transport in fibrous materials. Computer simulations based on this method realistically and quantitatively depict the dynamic liquid ascending wicking process. And, parametric study can be carried out to examine the influences of such important factors as fiber orientation on the transport behavior of liquid in the structure.

This meso-scale approach provides a bridge between the macro behavior of a material and the behaviors and interactions between its micro constituent particles. It is especially useful in the study of materials with characteristic length scale over the range of nano- and micro-meters, as it is reported that there is limitations of the continuum mechanics approach in describing the behavior of materials at scales smaller than tens of micros.

The multi-scale modeling of transport in fibrous materials is conducted in this paper, going through from quantum field theory, to statistical mechanics, and then to classical continuum methods. The transition from one scale to another is carried out by a so called "hand-shaking strategy," that is, the information gained from a lower scale is summed into a finite set of parameters, and passed onto the higher scale. Specifically, the Hamaker constant, which is required as an input for the Ising model, can be calculated from quantum field theory. Then, the predicted transport behavior of liquid in fibrous materials can be used to derive macroscopic parameters, such as the wicking rate K.

By means of discretizing the system in a lattice, this approach should be useful in studying material systems with complicated structures in nano scales. The size of the lattice is corresponding to the characteristic length of the system structure. Although the examples shown in this paper involved only fibrous system in microscales, it can be adapted to material systems in nanoscales by changing the lattice size/characteristic length in simulations.

Also, only nearest neighbors interact is considered in the present modeling, as the lattice size in the wicking simulation is in the scale of micros. Interactions of more distant term are therefore negligible. When the current approach is applied to material system in nanoscales and lattice size would be in the scales of nanometer, interactions of more distant terms should be accounted for. These terms may include second nearest neighbors and third neighbors, etc.

References

1. D. B. Abraham and C. M. Newman, Recent exact results on wetting. In *Lecture Notes in Physics*, edited by J. De Coninck and F. Dunlop, Springer-Verlag, Berlin, Heidelberg, New York (**1990**), Vol. 354, pp. 13–21.
2. F. Brochard and P. G. de Gennes, *J. Phys. Lett.* 45, L597 (**1984**).
3. P. K. Chatterjee, Absorbency, Elsevier, Amsterdam/NewYork, (**1985**).
4. P. G. De Gennes, *Rev. Modern Phys.* 57, 827 (**1985**).
5. V. E. B. Dussan and S. H. Davis, *J. Fluid Mech.* 65, 71 (**1974**).
6. N. M. Ghoniem and K. Cho, *CMES* 3, 147 (**2002**).
7. W. A. Goddard, T. Cagin, M. Blanco, N. Vaidehi, S. Dasgupta, W. Floriano, M. Belmares, J. Kua, G. Zamanakos, S. Kashihara, M. Iotov, and G. H. Gao, *Comput. Theor. Polym. Sci.* 11, 329 (**2001**).
8. Y. L. Hsieh, *Textile Res. J.* 65, 299 (**1995**).
9. C. Huh and L. E. Scriven, *J. Colloid Interf. Sci.* 35, 85 (**1971**).
10. J. N. Israelachvili, Intermolecular and Surface Forces, Academic Press, London (**1985**).
11. W. K. Krigbaum and J. V. Dawkins, Polymer Handbook, 2nd edn., Wiley, New York (**1975**).
12. D. Lukas, E. Glazyrina, and N. Pan, *J. Textile Inst.* 88, 149 (**1997**).
13. D. Lukas and V. Soukupova, Recent studies of fibrous materials wetting dynamics. In *INDEX 99 Congress*, R&D, Geneva (**1999**).
14. D. Lukas and N. Pan, *Polym. Comp.* 24, 314 (**2003**).
15. D. Lukas, V. Soukupova, N. Pan, and D. V. Parikh, *Simulation* 80, 547 (**2004**).
16. R. Lucas, *Kolloid Z.* 23, 15 (**1918**).
17. A. Lukkarinen, K. Kaski, and D. B. Abraham, *Phys. Rev. E* 51, 2199 (**1995**).
18. S. S. Manna, H. J. Herrmann, and D. P. Landau, *J. Stat. Phys.* 66, 1155 (**1992**).
19. K. M. Pillai and S. G. Advani, *J. Colloid Interf. Sci.* 183, 100 (**1996**).
20. V. M. Starov, S. A. Zhdannov, S. R. Kosvinstev, V. D. Sobolev, and M. G. Velarde, *Adv. Colloid Interf. Sci.* 104, 123 (**2003**).
21. E. W. Washburn, *Phys. Rev.* 17, 273 (**1921**).
22. W. Zhong, X. Ding, and Z. L. Tang, *Textile Res. J.* 71, 762 (**2001**).
23. W. Zhong, X. Ding, and Z. L. Tang, *Textile Res. J.* 72, 751 (**2002**).

Received: 13 August 2005. Accepted: 17 January 2006.